Evaluation of the ANX blast model in room acoustic simulations for assessing hearing load

Philipp Bechtel, Christian Kleinhenrich, Karl-Wilhelm Hirsch
Cervus Consult GmbH, bechtel@cervus.de

Abstract
To assess hearing load during handgun shooting, several factors must be considered, including the firearm, ammunition, hearing protection, and environment. Reflections from nearby surfaces are especially important alongside direct sound. Designing low-exposure shooting ranges therefore requires realistic gunshot simulations. Simulation quality depends on accurate source models, sound propagation, reflections and diffraction. In this study, the Chaser software with the ANX[1] source model and nonlinear propagation was used. Reflections were modeled with measured angle-dependent parameters and diffraction with UDFA[2]. The resulting sound signals were evaluated using hearing damage models such as AHAAH[3]. Validation was done by comparing simulations with real gunshot recordings from open and enclosed shooting ranges.

Previous studies
In 2025, two studies on the frequency and angular dependence of gunshots near the muzzle were presented. For this purpose, the direct sound components of synthesized and measured gunshots were compared on a circle with a radius of 10 m and an angular resolution of 10°. In the first paper[4], it was demonstrated that, using a Weber blast model[5] and directivity obtained via a two-stage cosine transformation, the hearing load at a muzzle distance of 10 m can be realistically predicted. In the second paper[6], the ANX[1] was considered as the source model, and a cosine transformation was also used as the directivity. By taking into account the nonlinear sound propagation of this source model, the hearing load could be realistically mapped not only at the measurement points on the 10 m circle but also at closer reference points.

ANX Source Model
This model was presented in 2024 by Salomons[1] under the title: *Analytical model for sound of explosives and firearms (ANX)*. It is based on a Friedlander blast[7] illustrated in Figure 1, which has two characteristic parameters: the peak sound pressure P and the positive transit time T.

The distinctive feature of the ANX model is nonlinear sound propagation. In this context, the peak sound pressure $P(r)$ and the duration of the positive N-wave flank $T(r)$ are distance-dependent quantities determined by Equations (3) and (4). As $T(r)$ increases, the spectral energy shifts to lower frequencies. This causes a result, the blast becomes lower in frequency as the distance from the muzzle increases. Using r_*, the energy is converted into a radius according to Equation (2).

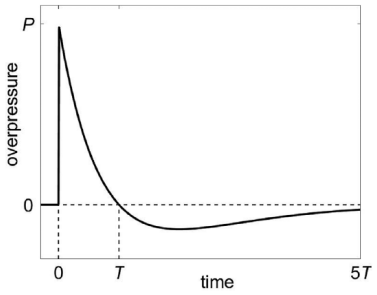

Figure 1: Friedlander waveform, with peak sound pressure P and positive N-wave flank T[1]

$$p(t) = P(r)\left(1 - \frac{t}{T(r)}\right)e^{-t/T(r)} \quad (1) \qquad r_* = 0.7\sqrt[3]{\frac{E}{\rho c^2}} \quad (2)$$

$$P(r) = K\rho c^2 \frac{r_*}{r}\sqrt{\frac{1}{\ln(r/r_*)}} \quad (3) \qquad T(r) = K\beta\frac{r_*}{c}\sqrt{\ln(\frac{r}{r_*})} \quad (4)$$

Table 1: Relevant constants and reference values

K	β	ρ	c	t_0	p_0
0.38	1.2	1.2 kg/m^3	340 m/s	1 s	20 µPa

Directivity
To account for the directional dependence of a shot, an angle-dependent source energy $E(\phi)$ is determined. Using the coefficients of the rifle considered here from Table 2, the angle-dependent source energy can be determined via the cosine transform according to Equation (5).

Table 2: Coefficients for determining the direction-dependent source energy of a rifle muzzle blast using the 5th order cosine transformation

Index i	1	2	3	4	5
c_i / J	2521	1908	557	79	52

$$E(\phi) = \sum_{i=1}^{N} c_i \cdot cos(\phi \cdot (i-1)) \quad (5)$$

Sound Propagation Calculation
The software tool *Chaser*, a mirror-source method, was used to calculate sound propagation. The points on surfaces used to calculate reflection and on edges used to determine diffraction components are determined based on the IEM *Image Edge Model*[8]. Reflections at surfaces are considered both frequency-dependent and broadband based on reflection classes according to [9, 10].

For frequency-dependent analysis, third-octave band-dependent reflection parameters measured in situ using near-field holography or DIN EN 1793-5 are used.

The UDFA *Universal Diffraction Filter Approximation*[2] models the diffraction components. In this model, cutoff frequencies and gain factors are determined from the geometric parameters of the edge as well as the incident and exit angles of the sound paths. A low-pass filter then uses these coefficients to form the frequency-dependent transfer function.

Facilities and microphone positions

This article examines three shooting range scenarios. The simplest is an open-field setup, where only a gravel surface reflects sound. There are no diffraction paths, so only the direct sound and ground reflection contribute.

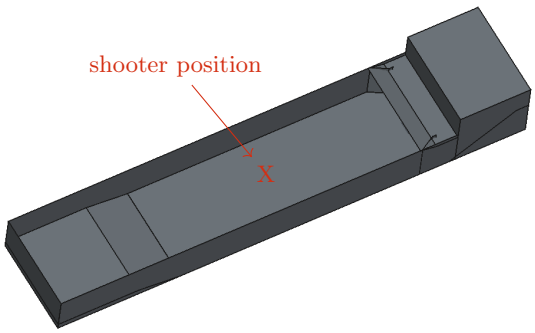

Figure 2: Model of the indoor shooting range with the ceiling hidden

The second scenario is an indoor range about 32 m long, 8 m wide, and 2.8 m to 3.3 m high. A sloped bullet trap at the front prevents first-order reflections from reaching the shooter. Due to a ramp, the ceiling height at the rear is reduced by about 0.5 m. Walls and ceiling are acoustically treated, and the floor is largely soundproof. The shooter is positioned in the front central area.

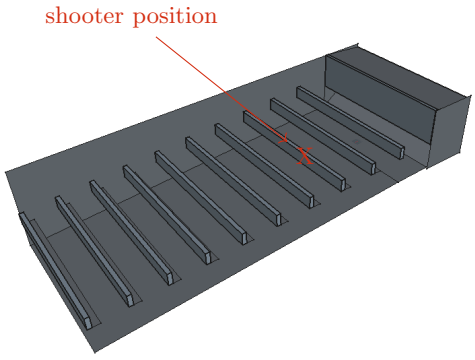

Figure 3: Model of the target area with the ceiling and side wall hidden

The third scenario examines a target area. This facility is 50 m long and 20 m wide, with a sloped bullet trap at the front and an open rear leading to the standing area. Joists span the width beneath the 5 m ceiling at regular intervals, reducing the clear height to 3.5 m. Walls, ceiling, and partitions are acoustically treated, while the ground is gravel. The shooter is positioned in the front central area below a joist.

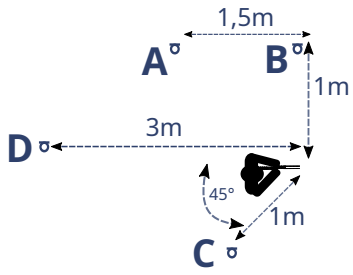

Figure 4: Sketch of measurement points
(Measurement point A is mirrored across the shooting axis)

Figure 4 shows the microphone positions used to record the shot signals for each shooter position. All measurement points have a height of 1.6 m. In simulations, the muzzle height was set to 1.4 m, while in measurements it varied between 1.27 m and 1.45 m m depending on the shooter's height.

Investigations

This section evaluates the ANX source model for predicting hearing load near the muzzle. The AHAAH model[3] , developed specifically for gunfire noise, is a validated method used by the United States military[11]. All calculations apply consistent settings: unwarned, no hearing protection, and frontal sound incidence.

For each facility type, four scenarios are analyzed, varying in diffraction effects and reflection parameter resolution. The abbreviations used are listed in Table 3.

Table 3: List of Abbreviations

RK	Broadband reflection classes[9, 10]
R(f)	Third-octave band reflection coefficients
NoDiffraction	Diffraction components are neglected
UDFA	Calculation of diffraction using UDFA[2]

In Figures 5 to 7, hearing load is shown for each facility and microphone position, based on measured and predicted values. Measured hearing load is displayed as a bar, with the top edge representing the 80th percentile and the bottom edge the 20th percentile of 10 shots The significant difference between these two percentiles is a well-known phenomenon in near-muzzle shot measurements[12]. The predicted hearing loads are displayed as colored markers.

Hearing Load from the Areas

Figure 5 shows the hearing loads in the open-field scenario. Predictions match the measured values well at microphone position A, slightly underestimate them at position B, and considerably underestimate them at positions C and D.

For the indoor range in Figure 6, predictions differ between broadband reflection classes and third-octave band-dependent parameters. Frequency-dependent reflection parameters reduce predicted hearing load by up

to 15 %. Diffraction effects have no noticeable impact. Predictions match measured values at positions A, B, and D, with underestimation only at position C.

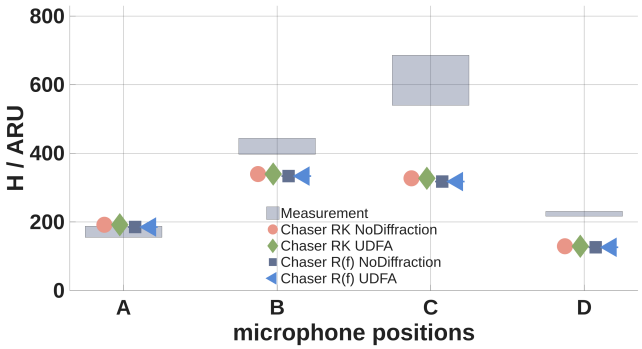

Figure 5: Open-field: hearing load following measurement and prediction at the respective measurement points

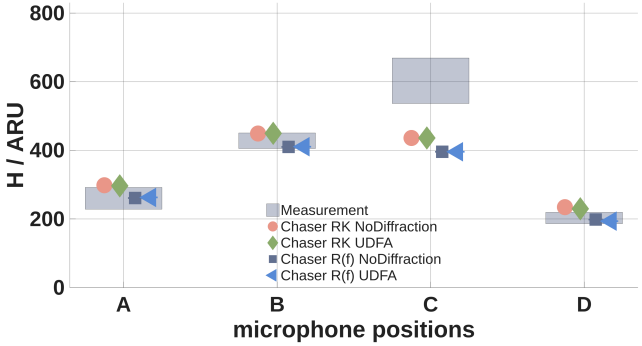

Figure 6: Indoor shooting range: Hearing load based on measurements and predictions at the respective measurement points

For the target area in Figure 7, prediction models show only minor differences. Scenarios with UDFA and broadband reflections yield hearing loads up to 3 % higher than models without diffraction or frequency-dependent reflections, while diffraction alone contributes at most 1 %. Predictions match measured values at position B, slightly underestimate at A, and significantly underestimate at C and D.

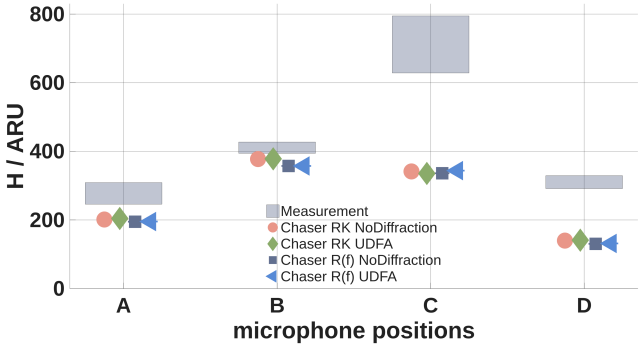

Figure 7: Target area: Hearing load based on measurements and forecasts at the respective measurement points

In summary, hearing load at points A and B was predicted accurately across all facilities. Predictions at point C were consistently too low, while at point D, realistic predictions were only achieved for the indoor range. Comparing measurements at point D shows substantial variability in the reference data. Based on facility geometry and surfaces, the indoor range would be expected to produce the highest hearing load and the open field the lowest. However, measured values were approximately ∼230 ARU, in the open field, ∼200 ARU, in the indoor range, and ∼320 ARU, in the target range. The cause can only be estimated and requires further investigation. Possible factors include the stature of each shooter[1] and resulting differences in muzzle height, as well as slight deviations of a few centimeters in the measurement setup.

Detailed Signal Analysis

Another potential reason for the discrepancy between measured and predicted results emerges from the analysis of the sound pressure time histories and frequency responses.

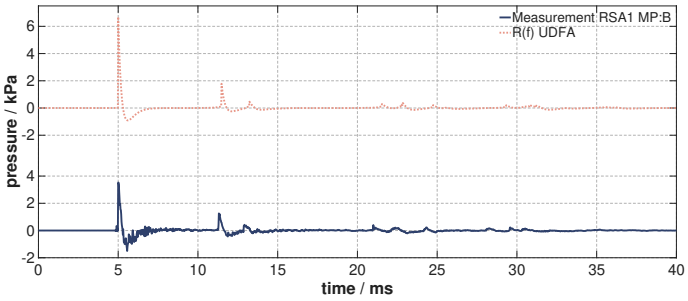

Figure 8: Indoor shooting range: Shifted sound pressure time histories at measurement point B

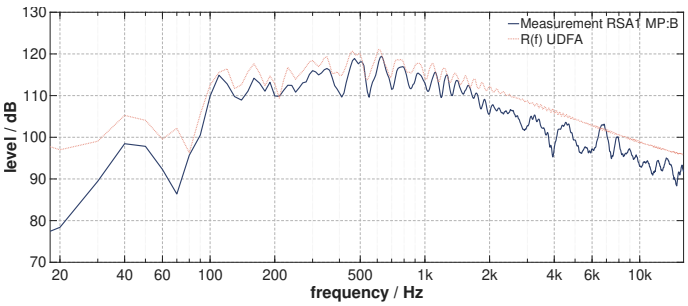

Figure 9: Indoor shooting range: Smoothed frequency responses at measurement point B

Figure 8 shows the measured and predicted sound pressure time history at point B in the indoor range, with corresponding frequency responses in Figure Figure 9. Both signals produce a hearing load of ∼400 ARU, despite a peak level difference of ∼6 dB. This occurs because the AHAAH model attributes only ∼20 % of the auditory load to the peak, with the remaining ∼80 % influenced by the rest of the signal[13]. The model also emphasizes frequencies between 1 kHz to 4 kHz. The ANX source model's tendency to overestimate higher-frequency components[6] also contributes to the observed peak level difference.

Figure 10 highlights the strong influence of signal shape on AHAAH model hearing damage predictions. Here,

[1] A different shooter was used at each range

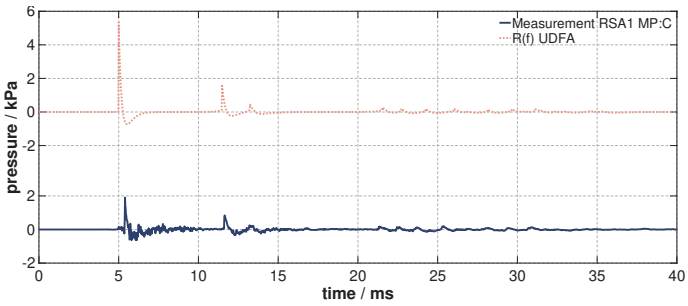

Figure 10: Indoor shooting range: Shifted sound pressure time curves at measurement point C

the measured hearing load is about 200 ARU higher than the predicted value, even though the simulated signal's peak exceeds the measurement by ∼9 dB. Despite the higher level, the predicted hearing load is lower, likely due to pronounced fluctuations in the measurement signal between 6 ms and 8 ms. These fluctuations, caused by the muzzle brake, increase with the shot angle and are largest opposite the shot direction.

Despite these fluctuations and level differences, the time histories show strong agreement in the first reflections. Likewise, the frequency responses between 100 Hz and 1.5 kHz display very similar patterns.

Conclusion

As previous studies indicate, the ANX source model's nonlinearity enables realistic prediction of hearing load near the muzzle, but only in about 50 % of cases here. Its tendency to overestimate high-frequency components can make peak levels too high. Nevertheless, predicted hearing loads match measurements due to the AHAAH model's complex processing. In short, the results are accurate even though the scaling is incorrect.

This is not disqualifying, since in fields like emission control, signal shapes are secondary to overall levels. Additionally, as the muzzle exit angle increases, the muzzle brake increasingly affects the signal. This is a factor not accounted for by the ANX model or any other source model known to the authors.

Beyond the evaluation of the ANX model, additional conclusions can be drawn. The signal waveforms show strong agreement, validating the sound propagation routines in the *Chaser* simulation software. Using broadband reflection classes instead of third-octave band-dependent parameters can change predicted hearing load by up to 15 %, making this a significant factor. In contrast, diffraction components affect hearing load by less than 1 % for the facilities and shooter positions considered, and are therefore negligible.

Acknowledgments

This work was supported by BAIUDBw GS II 2 and IUD I 5 of the German Ministry of Defense.

References

[1] E. M. Salomons. "Analytical model for sound of explosives and firearms". In: *The Journal of the Acoustical Society of America* 156.3 (Sept. 2024), pp. 2034–2044. ISSN: 0001-4966. DOI: 10.1121/10.0030301.

[2] C. Kirsch and S. D. Ewert. "Filter-based first- and higher-order diffraction modeling for geometrical acoustics". In: *Acta Acustica* 8 (2024), p. 73. ISSN: 2681-4617. DOI: 10.1051/aacus/2024059.

[3] P. D. Fedele et al. *Using the Auditory Hazard Assessment Algorithm for Humans (AHAAH) With Hearing Protection Software, Release MIL-STD-1474E.* Tech. rep. ARL-TR-6748. Army Research Laboratory, 2013.

[4] P. Bechtel et al. "Frequency- and Angle-dependent Source Models of Muzzle Blasts close to the Gun". In: *Proceedings of DAS—DAGA 2025.* Ed. by Deutsche Gesellschaft für Akustik e.V.(DEGA). 2025, pp. 798–801. ISBN: 978-3-939296-23-2. URL: https://pub.dega-akustik.de/DAS-DAGA_2025/files/upload/start/DAS-DAGA2025_proceedings_manuscripts.pdf.

[5] W. Weber. "Das Schallspektrum von Knallfunken und Knallpistolen mit einem Beitrag über die Anwendungsmöglichkeiten in der elektroakustischen Meßtechnik". In: *Akustische Zeitschrift* 4.6 (1939), pp. 373–391.

[6] P. Bechtel et al. "Two hybrid directivity models of muzzle blasts to describe the frequency and distance dependency". In: *Proceedings of the 11th Convention of the European Acoustics Association Forum Acusticum / EuroNoise 2025.* FA2025. European Acoustics Association, Dec. 2025, pp. 3117–3124. DOI: 10.61782/fa.2025.0922.

[7] F. G. Friedlander. "The diffraction of sound pulses I. Diffraction by a semi-infinite plane". In: *Proceedings of the Royal Society of London. Series A. Mathematical and Physical Sciences* 186.1006 (Sept. 1946), pp. 322–344. ISSN: 2053-9169. DOI: 10.1098/rspa.1946.0046.

[8] A. Erraji et al. "The image edge model". In: *Acta Acustica* 5 (2021), p. 17. ISSN: 2681-4617. DOI: 10.1051/aacus/2021010.

[9] F. Hammelmann et al. "Akustische Aspekte bei der Errichtung und Ertüchtigungen von Schießanlagen der Bundeswehr". In: *Fortschritte der Akustik.* Ed. by Deutsche Gesellschaft für Akustik (DEGA). Stuttgart, Mar. 2022.

[10] *Baufachliche Richtlinien Standortschießanlagen der Bundeswehr, Anhang 6: Anwendung Baulicher Lärmschutz für Schießanlagen der Bundeswehr – Grundlagen für die Berücksichtigung des Lärmschutzes beim Schießen mit Handwaffen.* Tech. rep. Version 1.0. Bundesministerium der Verteidigung, 2022.

[11] US Department of Defense. *MIL-STD-1474E: Design Criteria Standard Noise Limits.* Military Standard. 2015.

[12] C. Kleinhenrich et al. "Zur Reproduzierbarkeit von quellnahen Schießlärmmessungen zur Beurteilung des Gehörschädigungsrisikos". In: *Fortschritte der Akustik.* Ed. by Deutsche Gesellschaft für Akustik (DEGA). Stuttgart, Mar. 2022.

[13] G. R. Price. "Theoretical constraints on methods for rating auditory hazard from weapons-level sounds". In: *Proceedings of the 6th Convention of the European Acoustics Association Forum Acusticum.* U.S. Army Research Laboratory, Human Research and Engineering Directorate,Aberdeen Proving Ground MD 21005, USA. 2011, pp. 733–738.